AMSI
VACATION
RESEARCH
SCHOLARSHIPS
2018-2019

Dynamics of Compound Droplets

Eliza Jones
Supervised by Dr Anja Slim
Monash University

Vacation Research Scholarships are funded jointly by the Department of Education and Training and the Australian Mathematical Sciences Institute.

AMSI AUSTRALIAN MATHEMATICAL SCIENCES INSTITUTE

Australian Government
Department of Education and Training

Abstract

This paper aims to visualise the flow of magma around various objects through both numerical and analytic techniques. We analysed the flow around a sphere, spherical bubble, liquid droplet and compound droplet, gradually increasing the difficulty of the problem. Since magma is assumed to be Stokes flow, we are able to analyse the flow by defining a stream function, allowing us to visualise how the flow moves in space. To see how the flow moves in time, we numerically analysed the droplet using the single droplet code found in the Boundary Element Methods Library (BEMLIB) on MATLAB, (citation). This code visualises how a droplet deforms in time due to the flow around it by using the boundary integral method.

1 Introduction

Metal ores are formed in the earths crust, from metal-sulphide compounds in the Earths mantle, how these compounds are transported in magma remains poorly understood but is crucial in answering questions such as how far the magmatic sulphide liquid droplets can be transported in silicate melts, (Robertson *et al.*, 2016).

There are many theories behind transportation of these metal-sulphide liquid, which are widely assumed to be in droplet form. As the metal-sulphide liquid is known to be denser than the mafic magma, we need another solution for the transportation of these droplets to the Earths crust. A newly-postulated theory is through the use of compound droplets.

Compound droplets consist of a metal-sulphide liquid droplet with a spherical bubble cap. If the size ratio between the bubble cap and droplet is correct, then the compound droplet becomes buoyant, otherwise the droplet and bubble can deform and break apart. The compound droplets breaking apart is a consequence of many factors such as size, shape, and other constants such as Bond number and Reynolds number. The Bond number is a ratio of the gravitational forces to the surface tension forces whereas the Reynolds number is the ratio of inertial forces to viscous forces, (Roberston *et al.*, 2016).

Since we are working with mafic magma as our ambient (surrounding) fluid, due to its low Reynolds number and high viscosity we can assume our flow is Stokes flow. Stokes flow also known as creeping flow, is characterised by the very large viscosity μ and a slow velocity. This significantly reduces the difficulty of our problem, as we reduce the non-linear Navier-Stokes equation (1.1) to the linear Stokes equation (1.2) this means we are now assuming our flow is time independent and we can solve the

problem analytically. We solved by defining a stream function, which described the flows motion in space and how it interacted with certain objects.

To see how the objects, specifically the droplets and compound droplets shapes change and deform, when they are not assumed to be spherical, we used the BEMLIB code. This code uses a common method called the Boundary Integral Method, to track boundary elements on a droplet in our case, seeing how this element moves and is displaced. This allowed us to see how the droplets would deform and the conditions under which their shape would become stable and spherical, (Koh and Leal, 1989). In this paper, we only use this code for the single droplet case, the original idea was to create a similar code for the compound droplet case to see the dynamics of that system since it is still widely unknown, unfortunately due to the time constraints this did not happen.

This project involved recreating many previous works, as this problem of transporting compound droplets and their connection with to the formation of metal ores is an old theory, though as you can gather a lot about the dynamics is still unknown. This means my project is more educational for me, though in saying that I did recreate all of the following work and created the plots myself though using others codes.

1.1 Governing Equations

Navier-Stokes equations

$$\rho \frac{D\mathbf{v}}{Dt} = \rho g - \boldsymbol{\nabla} p + \mu \boldsymbol{\nabla}^2 \mathbf{v} \tag{1.1}$$

The Navier-Stokes equations are the main governing equation in fluid dynamics and are used in many fields with the ability to describe things from the weather to ocean currents. They can be extended to take into account temperature also, though for our use we only take into account the velocity, pressure and viscosity of the flow.

Stokes Equations

$$0 = -\boldsymbol{\nabla} p + \mu \boldsymbol{\nabla}^2 \mathbf{v} \tag{1.2}$$

The Navier-Stokes can be simplified to the Stokes equation, since we are working with mafic magma, a form of Stokes flow, meaning the viscosity forces dominates the inertial forces. Along with

the assumption of axisymmetry, this allows us to use the technique of defining a stream function which enables us to describe our flow analytically.

Continuity

We are using the continuity equation for an imcompressible flow, this means the flow has a constant density. For our purposes, the continuity equation is when the divergence of the velocity field equals zero.

$$\boldsymbol{\nabla}.\mathbf{v} = 0 \tag{1.3}$$

As we know that the flow is independent of ϕ, from continuity we can define our stream function ψ in terms of our velocity components v_r and v_θ

$$v_r = \frac{1}{r^2 \sin(\theta)} \frac{\partial \psi}{\partial \theta}$$
$$v_\theta = \frac{-1}{r \sin(\theta)} \frac{\partial \psi}{\partial r}$$

Ascent Velocity and Drag force

From the velocity components, we were able to find an expression for the ascent/terminal velocity by balancing the drag forces with the gravitational forces.

$$\Delta \rho V g = \iint \boldsymbol{\sigma}.n \; dS \tag{1.4}$$
$$\frac{4\Delta\rho\pi a^3 g}{3} = \iint \boldsymbol{\sigma}_{r\theta} \sin\theta + \boldsymbol{\sigma}_{rr} \cos\theta \; dS \tag{1.5}$$

Where $\sigma_{r\theta}$ is the shear stress, σ_{rr} is the full effective stress, ρ is the ambient fluid density and our volume was assumed to be and remain spherical.

2 Analysis of flow

2.1 Flow Around a Sphere

I found the stream function around a solid sphere, as done in Clift *et al,* (1978). The boundary conditions were that the tangential and normal velocity in terms of ψ were zero on the boundary of the sphere as seen below. The boundary conditions impose that we are assuming the sphere remains spherical (normal velocity = 0) and the tangential component imposes a no-slip condition meaning the fluid will have zero velocity relative to the boundary.

$$\frac{\partial \psi}{\partial r} = 0 \tag{2.1}$$

$$\frac{\partial \psi}{\partial \theta} = 0 \tag{2.2}$$

The far field velocity was set to $v = Uk$, since the flow is independent of ϕ (as we have assumed so swirling), in component form, $v_r = U\cos(\theta)$ *and* $v_\theta = -U\sin(\theta)$, thus using the governing equations found the stream functions had a general form of,

$$\psi = f(r)\sin^2(\theta) \tag{2.3}$$

$$\text{Where } f(r) = Ar^4 + Br^2 + Cr + \frac{D}{r} \text{ and a far field solution of } \psi = \frac{Ur^2\sin^2(\theta)}{2} \tag{2.4}$$

Using the three boundary conditions we were able to find the coefficients A, B, C and D. since the dominating term is of the far field solution is of order 2, this implies that $A = 0$ *and* $B = \frac{U}{2}$. From the remaining conditions and (2.3), in terms of the function f, we have that $f(a) = 0$ and $f'(a) = 0$, where a is the radius of the sphere. After some algebra we found that $C = \frac{-3}{4}Ua$ and $D = \frac{1}{4}Ua^3$.

Thus the stream function for a creeping flow around a solid sphere is,

$$\psi = \frac{U\sin^2(\theta)}{4}\left[2r^2 - 3ar + \frac{a^3}{r}\right]$$

The velocity components were also found,

$$v_r = U\left[1 - \frac{3a}{2r} + \frac{a^3}{2r^3}\right]\cos(\theta)$$

$$v_\theta = -\frac{U}{4}\left[4 - \frac{3a}{r} - \left(\frac{a}{r}\right)^3\right]\sin(\theta)$$

Using (1.5) we were able to find an expression for the ascent velocity of the sphere, this expression is a general one and relies on different parameters of the ambient fluid.

$$U_{ascent} = \frac{2\Delta\rho g a^2}{9\mu}$$

2.2 Flow around a Bubble

Using the same linear flow as in the sphere case, the flow around a bubble differs as we no longer have the tangential velocity equalling zero (no-slip condition) since we are assuming the fluid does not stick to the bubble. We instead introduce the condition where $\tau_\theta = \sigma_{r\theta} = 0$ at $r = a$, meaning the bubble can exert no tangential traction on the fluid.

As we have the same far field condition, and thus same far field solution as in the spherical case, we know the general form of the stream function for the bubble case will be the same. Therefore,

$$\psi = f(r)\sin^2(\theta)$$

As previously stated, we know that $f(r) = Ar^4 + Br^2 + Cr + \frac{D}{r}$, where $A = 0$ and $B = \frac{U}{2}$, where U is the far field characteristic velocity. Using the new boundary conditions we can find values for C and D in terms of B. The first condition, $v_r = 0$ implies that $f(a) = 0$, where a is the radius of the bubble.

$$f(a) = Ba^2 + Ca + \frac{D}{a} = 0$$
$$\text{Thus, } D = -Ba^3 - Ca^2$$

The second condition using the Cauchy stress tensor σ, we have that,

$$0 = \mu\left[\frac{1}{r}\frac{\partial v_r}{\theta} + r\frac{\partial}{\partial r}\left(\frac{v_\theta}{r}\right)\right]$$

After some algebra and substituting in the forms with $f(r)$ we find that,

$$0 = -\sin(\theta)\left[\frac{2f(r)}{r^3} + \frac{f''(r)}{r} - \frac{2f'(r)}{r^2}\right]$$

From this we find that, $\frac{6D}{a} = 0$, this implies that $D = 0$, thus our equation $f(r) = Br^2 + Cr$ and the first boundary condition becomes $0 = -Ba^3 - Ca^2$, thus $C = -Ba$. Therefore our equation f becomes, $f(r) = B(r^2 - ar) = \frac{U}{2}[r^2 - ar]$. Using this we found the final equation for ψ, v_r and v_θ, for when we have a bubble inside a creeping linear fluid.

$$\begin{aligned}
\psi &= \frac{Ur^2\sin^2(\theta)}{2}\left[1 - \frac{a}{r}\right] \\
v_r &= U\left[1 - \frac{a}{r}\right]\cos(\theta) \\
v_\theta &= \frac{-U}{2}\left[2 - \frac{a}{r}\right]\sin(\theta)
\end{aligned}$$

As in the sphere case we also calculated the ascent velocity of the bubble, though our drag force was significantly simplified due to the new boundary condition on the traction.

$$U_{ascent} = \frac{\Delta\rho g a^2}{3\mu}$$

2.3 Flow around a Droplet

The droplet scenario is best described as a fluid sphere, as inside the sphere is a fluid which is influenced by the movement of the outside fluid as it passes the sphere. In this scenario, we found two stream functions one for the outside fluid ψ (as done in the previous two parts), and a stream function for the droplet fluid ψ_d. Much of this analysis was based off of that done in the book Bubbles, Drops and Particles by R Clift, J Grace and M Weber, though a main difference was in the direction of our characteristic velocity.

As we have the same far field condition, we know the general form for $\psi = f(r)\sin^2(\theta)$, and by a consequence of the other boundary conditions at $r = a$, we know that $\psi_d = f_d(r)\sin^2(\theta)$. Where both

function f and f_d have the same general form as previously shown,$Ar^4 + Br^2 + Cr + \frac{D}{r}$.

The boundary conditions for this problem were found in Clift, Grace and Weber (1978) and are known to describe a spherical droplet. Again we have the no-slip condition, this reintroduces thus the tangential velocity of both fluids cannot be different at $r = a$,

$$\frac{\partial \psi}{\partial r} = \frac{\partial \psi_d}{\partial r} = 0$$

There is no flow across the interface, therefore at $r = a$ we have $\psi = \psi_d = 0$, this means we are assuming no mixing occurs between the two fluids. The next condition states the normal velocity is zero at $r = a$ for both fluids, this condition exists as it means we are assuming the droplet remains spherical, we will later look at the cases where deformation occurs. Thus,

$$\frac{\partial \psi}{\partial \theta} = \frac{\partial \psi_d}{\partial \theta} = 0$$

We also have that there is continuity in the tangential and normal stress components at the interface, thus our final boundary conditions are,

$$\frac{\partial}{\partial r}\left(\frac{1}{r^2}\frac{\partial \psi}{\partial r}\right) = \lambda \frac{\partial}{\partial r}\left(\frac{1}{r^2}\frac{\partial \psi_d}{\partial r}\right) \text{ on } r = a$$

$$p - 2\mu \frac{\partial}{\partial r}\left(\frac{1}{r^2 \sin(\theta)}\frac{\partial \psi}{\partial \theta}\right) + \frac{2\sigma}{a} = p_d - 2\mu_d \frac{\partial}{\partial r}\left(\frac{1}{r^2 \sin(\theta)}\frac{\partial \psi_d}{\partial \theta}\right) \text{ on } r = a$$

Where $\lambda = \frac{\mu_d}{\mu}$.

As previously shown, in ψ we have that $A = 0$ due to the far field condition (as $r \to \infty$). By a similar fashion, since we know that the stream function is finite and exists as $r \to 0$, we have that for ψ_d, $C_d = D_d = 0$, thus our stream function reduces to $\psi_d = A_d r^4 + B_d r^2$. We solved for the coefficients simultaneously by substituting in our functions of r, and knowing that $B = \frac{U}{2}$,

$$Ba^3 + Ca^2 + D = A_d a^5 + B_d a^3$$

$$2Ba^3 + Ca^2 - D = 4A_d a^5 + 2B_d a^3$$

$$-2Ba^3 - 2Ca^2 + 4D = 4\lambda A_d a^5 - 2\lambda B_d a^3$$

$$D = -Ba^3 - Ca^2$$

$$A_d = \frac{-B_d}{a^2}$$

Omitting the algebra, we found that,

$$B = \frac{U}{2}$$
$$C = \frac{-(2+3\lambda)Ua}{4(1+\lambda)}$$
$$D = \frac{U\lambda a^3}{4(1+\lambda)}$$
$$A_d = \frac{U}{4(1+\lambda)a^2}$$
$$B_d = -\frac{U}{4(1+\lambda)}$$

Thus our stream function for the flow around a droplet are,

$$\psi = \frac{Ur^2\sin^2(\theta)}{2}\left[1 - \frac{(2+3\lambda)a}{2r(1+\lambda)} + \frac{\lambda a^3}{2r^3(1+\lambda)}\right]$$
$$v_r = U\left[1 - \frac{(2+3\lambda)a}{2r(1+\lambda)} + \frac{\lambda a^3}{2r^3(1+\lambda)}\right]\cos(\theta)$$
$$v_\theta = \frac{-U}{2}\left[2 - \frac{(2+3\lambda)a}{2r(1+\lambda)} - \frac{\lambda a^3}{2r^3(1+\lambda)}\right]\sin(\theta)$$

The stream function for the fluid inside the droplet are,

$$\psi_d = -\frac{Ur^2\sin^2(\theta)}{4(1+\lambda)}\left[1 - \frac{r^2}{a^2}\right]$$
$$v_{r_d} = \frac{-U}{2(1+\lambda)}\left[1 - \frac{r^2}{a^2}\right]\cos(\theta)$$
$$v_{\theta_d} = \frac{U}{4(1+\lambda)}\left[2 - \frac{4r^2}{a^2}\right]\sin(\theta)$$

The ascent velocity of the droplet was found, where we have μ is the viscosity of the ambient fluid. As you can see this expression looks very similar to the spheres ascent velocity.

$$U_{ascent} = \frac{2\Delta\rho g a^2(1+\lambda)}{3\mu(2+3\lambda)}$$

2.4 Flow around a Compound Droplet

Our original plan was to follow on and see if we could code a compound droplet deforming in space, though this unfortunately had to be changed since we realised we would have to completely rewrite

the entire code which would take us far too long. So instead, we decided to analyse the compound droplet in a similar fashion to how we analysed the sphere, bubble and droplet by defining a stream function.

Our analysis in this section is based off of two papers, the 1997 paper by Khuri and Wazwaz and the 1989 paper by Vuong and Sadhal. These papers outline the details, but all analysis was done by hand. For this analysis, we used the toroidal cylindrical coordinate system, as it is considered the 'natural' coordinate system for this problem (Masoud and Felske, 2008). From Khuri and Wazwaz (1997) we were able to use a transform from cylindrical coordinates and derive the appropriate operator.

The transformation we used was,

$$z = R\frac{\sin\eta}{\cosh\xi - \cos\eta}$$
$$r = R\frac{\sinh\xi}{\cosh\xi - \cos\eta}$$

Where R is a scaling factor, which changes the radius of the sphere and torus in the coordinate systems, though the system is independent of this. Our operator in cylindrical coordinates differs from the Laplacian due to how the stream function is defined, though our new functions still satisfies the Stokes equations. This operator is labelled E.

$$E^4\psi = 0$$
$$E^2 = wh^2\left[\frac{\partial}{\partial\xi}\left(\frac{1}{w}\frac{\partial}{\partial\xi}\right) + \frac{\partial}{\partial\eta}\left(\frac{1}{w}\frac{\partial}{\partial\eta}\right)\right]$$

Where the variables w and h are equal to,

$$w = R\frac{\sinh\xi}{\cosh\xi - \cos\eta},\ h = \frac{\cosh\xi - \cos\eta}{R}$$

These substitutions were made for simplification. We now substitute in our general form of the stream function ψ such that $\psi = k(\xi,\eta)v(\xi,\eta)$, where v is an unknown function and

$$k(\xi,\eta) = R\frac{\sinh\xi}{(\cosh\xi-\cos\eta)^{\frac{3}{2}}}$$

Therefore we get the general form of $E^2\psi$ in terms of v and k,

$$\begin{aligned}E^2\psi = kh^2(v_{\xi\xi}+v_{\eta\eta}) + wh^2\left[\left(\frac{k}{w}\right)_\xi + \left(\frac{k_\xi}{w}\right)\right]v_\xi \\ + wh^2\left[\left(\frac{k}{w}\right)_\eta + \left(\frac{k_\eta}{w}\right)\right]v_\eta + wh^2\left[\left(\frac{k_\xi}{w}\right)_\xi + \left(\frac{k_\eta}{w}\right)_\eta\right]v\end{aligned}$$

This simplifies to

$$E^2\psi = \frac{1}{R}\sinh\xi(\cosh\xi-\cos\eta)^{\frac{-1}{2}}Lv = \bar{k}(\xi,\eta)Lv$$

Where,

$$\begin{aligned}Lv &= A(v_{\xi\xi}+v_{\eta\eta}) + Bv_\xi + Cv_\eta + Dv \\ \bar{k}(\xi,\eta) &= \frac{1}{R}\sinh\xi(\cosh\xi-\cos\eta)^{\frac{-1}{2}}\end{aligned}$$

Substituting this form into $E^2(E^2\psi) = 0$ we get the final operator E

$$\begin{aligned}0 = \frac{\bar{k}}{w}((Lv)_{\xi\xi}+(Lv)_{\eta\eta}) + \left[\left(\frac{\bar{k}}{w}\right)_\xi + \left(\frac{\bar{k}_\xi}{w}\right)\right](Lv)_\xi \\ + \left[\left(\frac{\bar{k}}{w}\right)_\eta + \left(\frac{\bar{k}_\eta}{w}\right)\right](Lv)_\eta + \left[\left(\frac{\bar{k}_\xi}{w}\right)_\xi + \left(\frac{\bar{k}_\eta}{w}\right)_\eta\right]Lv\end{aligned}$$

All the algebra from this process has been omitted for conciseness, if you would like to see the full derivation of this operator and eventually the general form of the stream function for the compound droplet please refer to Khuri and Wazwaz (1997) paper where the full derivation is outlined. The two papers I was following had slightly different general forms for the stream functions, arising from the different definitions of the stream functions and how the two papers non-dimensionalised their variables. The general form below is from the Vuong and Sadhal (1989) paper, this is the form I would use if I were to continue with this analysis.

$$\psi(\xi,\eta) = \frac{1}{(\cosh\xi - \cos\eta)^{\frac{3}{2}}}\Phi$$
$$= \frac{1}{(\cosh\xi - \cos\eta)^{\frac{3}{2}}}\int_0^\infty \hat{\phi}(\eta,\lambda)\sinh\xi^2 P'_{-\frac{1}{2}+i\lambda}(\cosh\xi)\ d\lambda$$

Where,

$$\hat{\phi}(\eta,\lambda) = \cos\eta[A^*(\lambda)\cosh\lambda\eta + B^*(\lambda)\sinh\lambda\eta]$$
$$+ \sin\eta[C^*(\lambda)\cosh\lambda\eta + D^*(\lambda)\sinh\lambda\eta]$$

This analysis has not been fully completed, I was able to fully define the general form of the stream function, though did not have time to find all the coefficients for the functions, as was done in Vuong and Sadhal (1989) paper. As we are now dealing with a bubble and droplet, this means we would define two stream functions, due to the differing η between the boundaries and the two different flows involved.

3 Numerically Analysing a liquid-sulphide droplet

3.1 Finding an appropriate Capillary Number

The Capillary number is a dimensionless ratio between the viscous and the surface tension forces on the droplet. For a droplet, we have to take into account the ratio of the droplet viscosity to the magma viscosity as seen in, Robertson *et al.*, (2016) which explains that for 'straining' flows' similar to our flow, the critical Capillary number will occur when,

$$Ca^* \approx 0.501\left(\frac{\mu_d}{\mu_m}\right)^{\frac{-2}{3}}$$

As we know that the viscosity of the surrounding magma is greater than the viscosity of the droplet, from Robertson *et al,* (2016), I was able to find values for the viscosity of the sulphide droplets (Copper and Iron) and three types of magma Komatiite, Basalt and Dacite. These three types of magma have varying viscosity's of 1, 100 and 1×10^4 Pa s respectively and the sulphide droplets had a viscosity of 2×10^{-2}. The critical Capillary numbers were calculated in Mathematica, and I found that Komatiites was 6.8, Basalt was 146.4 and Dacites was 3156.1. These values are realistic, but we will normally see Capillary numbers of much less than this. This implies that most of the droplets formed, particularly

in Dacite and Basalt magmas would be relatively stable.

Using the formula for the ascent/terminal velocity of the droplet, I calculated an approximate Capillary number for each of the three magma types. The Capillary number formula is,

$$Ca = \frac{\mu U}{\sigma}$$

Where μ is the ambient viscosity, σ is the droplet surface tension and U in our case is the ascent velocity, normally you use the characteristic velocity but using the terminal still gives us a good estimation. I approximated the droplet radius to be $1mm$, which is standard size for these droplets according to Robertson *et al,* (2016). Using these approximations, I again calculated three Capillary numbers for the different magmas, with Komatiite being 0.0149, Basalt being 0.0152 and Dacite being 0.0153, as you can see these values are very similar for the $1mm$ droplet. As the radius increases so would the Capillary number and the droplet would become less stable.

3.2 Plotting the droplet using BEMLIB

The Boundary Element Method Library is a collection of codes created by Costas Pozrikidis which is widely used in fluid dynamics. The codes use different methods for numerically analysing different flows, with all the software being free to use. For this project we used the drop_ax directory, which is for flow past an axisymmetric flow.

This section consists of images from the Matlab program used to plot the droplet as moves and shape changes throughout time. The way the droplet moved/deformed is dependent on the bond number and radius. I do note that this program will only go to the point of when breaking would occur but could not actually show what happens after the droplet breaks. The program used was the single_drop.m file which is the dynamics for the single droplet case which was explored earlier analytically. This process was based off the Koh and Leal (1989) paper which explored the different ways the droplets deformed through trial and error, though they used the parameter of a Reynolds number compared to the Bond number used in our code.

There are two main shapes, the prolate and oblate ellipsoids. Prolate shape is categorised by the major axis being vertically whereas the oblate shape major axis is horizontally, as seen below, with

their behaviour being very different when the fluid acts on them.

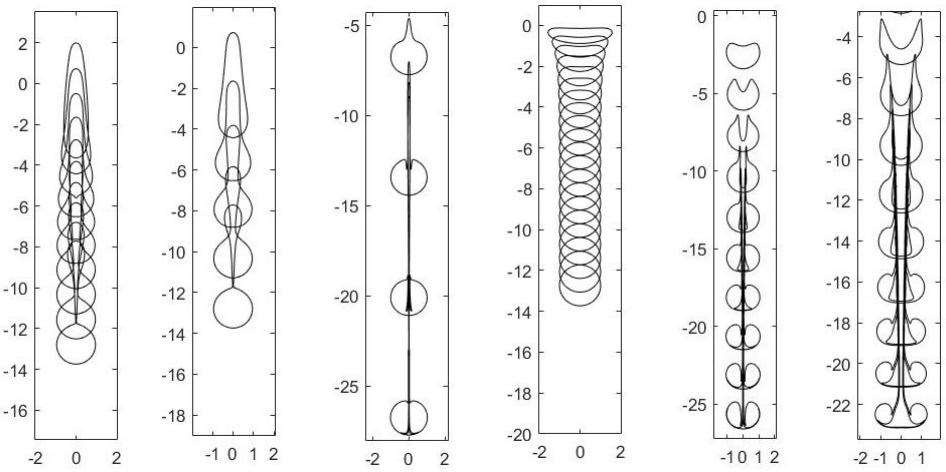

Figure 1: Depicts various droplet sizes with varying Bond numbers. The first three (a,b,c) depict prolate droplets with radius and Bond numbers of 0.55-2.86, 0.85-2.86 and 0.95-181 respectively. As you can see these all deform slightly differently and at different rates, with the least spherical deforming the fastest. Figures (a) and (b) deform similarly due to the same bond number, but you can see that (a) tails is significantly larger than (b). Figure (c) tail is very thin and long, though you can see this has cause some deformation inside the actual droplet, which is not common. Figure (c) may be an example of capillary waves appearing, though wave like structures were not detected. The second three (d,e,f) are examples of oblate droplets with radius and Bond numbers of 1.85-3.34, 1.15-181 and 1.55-181. For figure (d), this is the only example showing an initial ellipsoid droplet becoming spherical again, since the Bond number is small enough so this can occur. Figures (e) and (f) are both examples of the ring scenario where the cavity is large enough that a ring would form. In (f) we can assume this ring will eventually break off into two droplets, though it is hard to tell where in (e) the two droplets will break off or if they will reform.

Since the prolate shape is a 'longer' ellipsoid, as the fluid moved past the droplet, the shape would elongate, stretching out to form a tail. We can see this in figure 1(a), 1(b) and 1(c) which are prolate shapes of varying lengths. As you can see, the prolate shape will always form a small tail or 'spike' even if the shape over time reverts to spherical. As the ellipsoid gets long, the tail formed is wider, as increased volume of the shape is pushed away from the initial shape, we can infer that after the tail breaks away from the initial shape, the two individual shapes would both become spherical. Under certain conditions, one which I unfortunately was not able to plot, the tail could form Capillary waves,

this occurs if the drop is very viscous meaning it would not permit break off, (Koh and Leal, 1989). As studied by Stone and Leal (1989), once the amplitude of the Capillary waves becomes finite, the tail will break apart into different individual droplets.

The oblate shape is a wide ellipsoid, when a flow moves past the oblate shape, the ends curl around and become pointed. This makes a cavity on one side of the ellipsoid, where if the deformation is stable, this cavity will be filled in and the ellipsoid will become spherical again as seen in figure 1(d). As the ellipsoid becomes wider the cavity size increases, for some cases if the cavity is not too big a bubble can be formed inside the droplet, eventually though this bubble will escape and the process will be repeated. Otherwise, as seen above in 1(f) and 1(e), the cavity can become so large that the droplet can form a ring like shape, this ring shape is not stable though, since we know the droplet will want to be of minimum surface area, and thus want to form a sphere. From this, we can infer the ring would break up into two droplets after some time, since the 'cavity' or hole would be large such that the ring could not form back into one spherical shape. Since for this project we were not varying the viscosity of the droplet and were assuming our droplet was sufficiently viscous, though there is some evidence that wave like behaviour can occur in oblate shapes also though for droplets with low viscosity compared to the ambient fluid, (Koh and Leal, 1989).

4 Conclusion

Through analysing the flow around the sphere, bubble, liquid droplet and compound droplet we are able to find functions describing the flows motion around these objects in space. For the droplet we were able to do this using the BEMLIB code, allowing us to see how under different circumstances the droplets shape would deform and change. To further this project, would be to complete the analysis of the compound droplet, and then to create and eventually be able to plot the compound droplet in a similar way to the droplet. As we still do not know much about what is needed for the compound droplets to be buoyant and the conditions under which they will maintain their shape. This code will allow us to see the dynamics of the compound droplets, giving us further information about how the metal-sulphide droplets are transported in magma which is still widely unknown.

Bibliography

- Clift R, Grace J R, Weber M E, (1978). *Bubbles, Drops and Particles*, New York, Academic Press.
- Koh C J, and Leal L G, (1989). 'The stability of drop shapes for translation at zero Reynolds number through a quiescent fluid', *Physics of Fluids*, 1(8), pp. 1309-1313
- Khuri S A, Wazwaz A M, (1997). 'On the solution of a Partial Differential Equation', *Applied Mathematics and Computation*, 85, pp. 139-147
- Masoud H, Felske J, (2009). 'Analytical solution for Stokes flow inside an evaporating sessile drop: Spherical and cylindrical cap shapes', *Physics of Fluids*, 21 pp. 3-11
- Robertson J C, Barnes S J, Le Vaillant M, (2016). 'Dynamics of Magmatic Sulphide Droplets during Transport in Silicate Melts and Implications for Magmatic Sulphide Ore Formation', *Journal of Petrology*, 56(12), pp. 2445-2472
- Stone H A, and Leal L G, (1989). 'Relaxation and breakup of an initially extended drop in an otherwise quiescent fluid', *Journal of Fluid Mechanics*, 198, pp. 399-427
- Vuong S T, Sadhal S S, (1989). 'Growth and translation of a liquid-vapour compound drop in a second liquid. Part 1. Fluid mechanics', *Journal of Fluid Mechanics*, 209, pp. 617-637

Appendix

Appendix A: Boundary Integral Method

Solving Laplace's Equation

I first had to derive an expression for $p(x_0)$ in terms of our boundary conditions, given that we know p is a solution for Laplace's Equation so $\nabla^2 p = 0$. This was done using known vector calculus and identities. Our boundary conditions are the known Dirichelt and the Neumann conditions of,

$$p \text{ is given on the boundary } \partial D$$
$$\boldsymbol{\nabla} p = \frac{\partial p}{\partial n} \text{ is given on the boundary } \partial D$$

Where D is an arbitrary volume with the boundary of ∂D.

We define a variable $F = \nabla.(pq)$, where q is a green's function such that $\Delta q = \delta(x - x_0)$. Taking the divergence of F, we have our two separate expressions, $\nabla.F = q\Delta p - p\Delta q$. Thus we can use Green's second and third identities to find an expression for $p(x_0)$.

$$\int_D \boldsymbol{\nabla}.F \; dV = \int_{\partial D} F.n \; dA$$
$$\Rightarrow \int_D q\Delta p - p\Delta q \; dV = \int_{\partial D} q\boldsymbol{\nabla} p.n - p\boldsymbol{\nabla} q.n \; dA$$

using Green's Third identity for the function q, we can simplify our expression to,

$$\int_D q(x, x_0)\Delta p \; dV - p(x_0) = \int_{\partial D} q(x, x_0)\frac{\partial p(x)}{\partial n} - p(x)\frac{\partial q(x, x_0)}{\partial n} dA$$

Since we have that $p(x)$ is a solution to the Laplace equation we can simplify accordingly and thus find a solvable expression for $p(x_0)$ as we know $p(x)$ and $\frac{\partial p(x)}{\partial n}$ on the boundary.

$$p(x_0) = \int_{\partial D} p(x)\frac{\partial q(x, x_0)}{\partial n} - q(x, x_0)\frac{\partial p(x)}{\partial n} dA$$

Verifying Lorentz Reciprocal Theorem

The generalised Lorentz Reciprocal Theorem states that,

$$\int_S n.(v^{'}.\sigma - v.\sigma^{'})\ dS = \int_V v.(\boldsymbol{\nabla}.\sigma^{'}) - v^{'}.(\boldsymbol{\nabla}.\sigma)\ dV$$

Which consists of two Stokes flow in the same spatial domain with velocity and stress tensor (v, σ) and $(v^{'}, \sigma^{'})$ respectively. Where both velocities satisfy the continuity.

We define our terms as,

$$\sigma_{ij} = -p\ \delta_{ij} + 2\mu\ e_{ij} \tag{4.1}$$

$$e_{ij} = \frac{1}{2}(\partial_j v_i + \partial_i v_j) \tag{4.2}$$

$$\partial_j \sigma_{ij} = 0\ (S.C) \tag{4.3}$$

$$\partial_i v_i = 0\ (S.C) \tag{4.4}$$

$$\tag{4.5}$$

The last two equations are summations written in Einstein convention. These are the same for the equivalent flow, with both flows defined on the same domain V and boundary S. We start by multiplying 4.1 by $e^{'}_{ij}$ and $4.1^{'}$ by e_{ij}, where the $'$ denotes the equivalent flow.

$$\sigma_{ij}e^{'}_{ij} = -p\ \delta_{ij}e^{'}_{ij} + 2\mu\ e_{ij}e^{'}_{ij} \tag{4.6}$$

since

$$\delta_{ij}e^{'}_{ij} = e^{'}_{ii} = \partial_i v_i = 0 \tag{4.7}$$

$$\sigma_{ij}e^{'}_{ij} = 2\mu\ e_{ij}e^{'}_{ij} \tag{4.8}$$

Thus,

$$\mu^{'}\sigma_{ij}e^{'}_{ij} = \mu\ \sigma^{'}_{ij}e_{ij} \tag{4.9}$$

since the stress tensor is symmetric, $\sigma_{ij} = \sigma_{ji}$ and $\sigma^{'}_{ij} = \sigma^{'}_{ji}$ and

$$\sigma_{ij}e^{'}_{ij} = \frac{1}{2}\sigma_{ij}\partial_j v^{'}_i + \frac{1}{2}\sigma_{ij}\partial_i v^{'}_j = \sigma_{ij}\partial_j v^{'}_i = \partial_j(\sigma_{ij}v^{'}_i) - v^{'}_i\partial_j\sigma_{ij} \tag{4.10}$$

$$\sigma^{'}_{ij}e_{ij} = \frac{1}{2}\sigma^{'}_{ij}\partial_j v_i + \frac{1}{2}\sigma^{'}_{ij}\partial_i v_j = \sigma^{'}_{ij}\partial_j v_i = \partial_j(\sigma^{'}_{ij}v_i) - v_i\partial_j\sigma^{'}_{ij} \tag{4.11}$$

From equation 3 we can reduce 10 and 11 to

$$\sigma_{ij}e'_{ij} = \partial_j(\sigma_{ij}v'_i) \tag{4.12}$$

$$\sigma'_{ij}e_{ij} = \partial_j(\sigma'_{ij}v_i) \tag{4.13}$$

Substituting these results into, we find that

$$\mu'\partial_j(\sigma_{ij}v'_i) = \mu\partial_j(\sigma'_{ij}v_i) \tag{4.14}$$

$$\tag{4.15}$$

We can translate this into general tensor form,

$$\mu'\boldsymbol{\nabla}.(\sigma.v') = \mu\boldsymbol{\nabla}.(\sigma'.v)$$

Integrating over V, we have

$$\mu' \int_V \boldsymbol{\nabla}.(\sigma.v')\ dV = \mu \int_V \boldsymbol{\nabla}.(\sigma'.v)\ dV$$

Applying the divergence theorem we find

$$\mu' \int_S n.(\sigma.v')\ dS = \mu \int_S n.(\sigma'.v)\ dS$$

For this particular problem we have $\mu = \mu'$, thus we can rewrite these as

$$\int_V \boldsymbol{\nabla}.(\sigma.v') - \boldsymbol{\nabla}.(\sigma'.v)\ dV = \int_S n.(\sigma.v') - n.(\sigma'.v)\ dS$$